HHS Public Access

Author manuscript

Cancer Cell. Author manuscript; available in PMC 2017 October 10.

Published in final edited form as:

Cancer Cell. 2016 October 10; 30(4): 623–636. doi:10.1016/j.ccell.2016.08.015.

Discovery of dual inhibitors of MDM2 and XIAP for cancer treatment

Lubing Gu[1,4], **Hailong Zhang**[1,4], **Tao Liu**[1,4], **Sheng Zhou**[3,4], **Yuhong Du**[2], **Jing Xiong**[3], **Sha Yi**[1], **Cheng-Kui Qu**[1], **Haian Fu**[2], and **Muxiang Zhou**[1,*]

[1]Department of Pediatrics and Aflac Cancer and Blood Disorders Center, Emory University School of Medicine, Atlanta, Georgia 30322, USA

[2]Department of Pharmacology and Emory Chemical Biology Discovery Center, Emory University School of Medicine, Atlanta, Georgia 30322, USA

[3]Institute of Pathology, Tongji hospital, Tongji Medical College, Huazhong University of Science and Technology, Wuhan 430030, China

SUMMARY

MDM2 and XIAP are mutually regulated: Binding of MDM2 RING protein to the IRES region on XIAP mRNA results in MDM2 protein stabilization and enhanced XIAP translation. In this study, we developed a protein-RNA fluorescence polarization (FP) assay for high-throughput screening (HTS) of chemical libraries. Our FP-HTS identified eight inhibitors that blocked the MDM2 protein-XIAP RNA interaction, leading to MDM2 degradation. The compound-induced MDM2 downregulation resulted not only in inhibition of XIAP expression, but also in activation of p53, which contributed to cancer cell apoptosis in vitro and inhibition of cancer cell proliferation in vivo. Importantly, one of the MDM2/XIAP inhibitors, MX69, showed minimal inhibitory effect on normal human hematopoiesis in vitro and was very well tolerated in animal models.

In brief

Gu et al. use chemical screening to identify inhibitors of the MDM2 protein-XIAP mRNA interaction and show these inhibitors lead to apoptosis by reducing XIAP protein, decreasing MDM2 stability, and increasing p53 levels. Animal testing of one of these compounds shows anti-tumor efficacy and minimal toxicity.

*Correspondence: mzhou@emory.edu.

[4]Co-first author

Communications to: Muxiang Zhou, M.D., Division of Hematology/Oncology, Department of Pediatrics, Emory University School of Medicine, 1760 Haygood Drive, Atlanta, GA 30322, U.S.A., Telephone: 404-727-1426, Fax: 404-727-4455, mzhou@emory.edu

AUTHOR CONTRIBUTIONS

M.Z. conceived the project, designed the experiments and wrote the manuscript; L.G., H.Z., T.L. and S.Z. designed and performed most of the experiments including FP-HTS, binding and ubiquitination assays, polysome profiling, pathology and animal studies; J.X. and S.Y. performed cell culture, Western blot, WST cytotoxic analysis and flow cytometry studies. Y.D., C.Q. and H.F provided technique support and chemical libraries for FP-HTS.

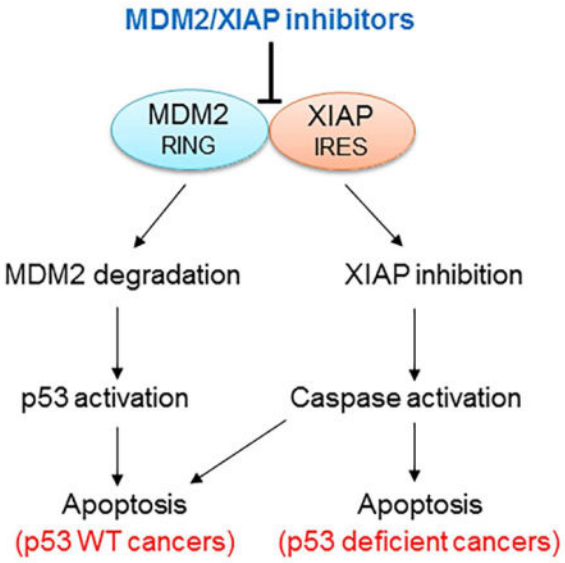

INTRODUCTION

The MDM2 protein has been extensively studied as an oncogene product that plays a critical role in cancer cell survival and disease progression. Elevated MDM2 protein expression has been documented in a large variety of human cancers and is thought to result from gene amplification as well as transcriptional and post-translational regulation. The best-characterized downstream target of MDM2 is p53. The N-terminus of the MDM2 protein binds to p53, inhibiting p53-mediated transcription (Momand et al., 1992). Furthermore, the MDM2 C-terminus acts as an E3 ubiquitin ligase, mediating the degradation of p53 (Haupt et al., 1997). Small-molecule inhibitors of MDM2 such as nutlin-3 and HLI98, which block MDM2-p53 interaction and inhibit the ubiquitin ligase activity of MDM2 respectively, have been actively investigated in preclinical studies and clinical trials for the treatment of cancer (Ray-Coquard et al., 2012; Yang et al., 2005).

In addition to acting as an E3 ubiquitin ligase, the C-terminal RING domain of MDM2 is able to bind mRNA and regulate gene expression. For example, the RING domain of MDM2 can bind to p53 mRNA and promote its translation (Candeias et al., 2008). Additional studies, including those from our group, demonstrated that the MDM2 RING domain binds to mRNAs of XIAP, VEGF, MYCN and Slug to regulate their translation in cancer cells, thus playing several p53-independent roles in cancer pathogenesis (Gu et al., 2012; Gu et al., 2009; Jung et al., 2013; Zhou et al., 2011). Specifically, we have shown that, in response to radiation, MDM2 protein is translocated from the nucleus to the cytoplasm. In the cytoplasm, MDM2 binds to XIAP-IRES mRNA and positively regulates IRES-dependent XIAP translation, leading to cancer cell resistance to radiation-induced apoptosis (Gu et al., 2009).

XIAP, an important member of the IAP family, has been well characterized to specifically inhibit caspases 3, 7 and 9, the enzymes that induce the mitochondrial apoptotic pathway. The mitochondrial apoptosis pathway is the major cell-death mechanism induced by

radiotherapy and many chemotherapeutic drugs (Schimmer, 2004). Specific inhibition of these caspases by the XIAP protein suggests that XIAP is crucial for the development of resistance to anticancer treatment. In fact, previous studies have shown that elevated expression of XIAP is detected in various types of cancer, and that a high level of XIAP expression is related to chemotherapy resistance and poor outcome (Berezovskaya et al., 2005; Mizutani et al., 2007; Tamm et al., 2004). XIAP expression is mainly regulated by an IRES-mediated mechanism at the translational level (Holcik et al., 1999). The IRES-mediated translation of XIAP is specifically activated when cells undergo cellular stress, such as exposure to radiation or treatment with chemotherapeutic drugs (Lewis and Holcik, 2005). The activation of XIAP IRES by the MDM2 RING protein, which is localized in the cytoplasm after exposure to radiation, supports this notion.

On the other hand, the E3 ubiquitin-ligase activity of the MDM2 RING protein is regulated by binding of XIAP IRES mRNA, as reported in our recent publication (Liu et al., 2015). It has previously been shown that mRNA binding can positively regulate expression of MDM2 protein. Specifically, binding of p53 mRNA to the MDM2 RING domain increases MDM2 expression (Candeias et al., 2008). Our studies further determined that the XIAP IRES-mediated increase in MDM2 protein expression is through inhibition of MDM2 homodimerization; this results in a reduction of the E3 ubiquitin ligase activity of the C-terminal RING domain by which MDM2 targets itself for ubiquitination and degradation (Liu et al., 2015).

Thus, our studies suggest that binding of XIAP IRES to the MDM2 RING domain simultaneously increases expression of MDM2 and XIAP, enhancing cancer progression and resistance to apoptosis. Accordingly, we hypothesized that inhibition of the molecular interaction between XIAP IRES and MDM2 RING domain would result in a simultaneous decrease in the expression of MDM2 and XIAP, leading to both anti-proliferative and enhanced-apoptosis effects. The present study was designed and carried out to test these hypotheses.

RESULTS

Development of FP assay and performance of HTS

In order to identify reagents or small-molecule compounds that could block the binding between XIAP IRES and the MDM2 RING domain, we developed an FP assay for use in HTS. First, we performed in vitro transcription to synthesize a 50-nt RNA fragment that covers the XIAP IRES sequence and then labeled it with fluorescein. Optimization analysis showed that at greater than 1 ng/ml of RNA-fluorescein, the tracer signal was more than 10 times greater than the background (buffer) (Figure 1A), resulting in a constant tracer signal of approximately 100 mP (Figure S1A). Next, we performed FP to test for binding between the fluorescent XIAP RNA probe and the GST-fused MDM2 RING protein. At the optimized RNA concentration of 1 ng/ml, there was a direct correlation between fluorescent RNA binding and amount of MDM2 RING protein added. Polarization progressively increased until reaching saturation (Figure 1B). At these concentrations, fluorescent XIAP IRES bound well to MDM2 RING protein, resulting in an assay window of approximately 80 mP and a K_d value of 6.6 μg/ml. Consistent with results obtained by UV cross-linking of

isotope-labeled probes (Gu et al., 2009), a similar-sized fluorescence-labeled control XIAP RNA copied from the upstream region of the XIAP IRES sequence did not bind to the MDM2 RING protein (Figure S1B). Also, the XIAP IRES did not bind to MDM2 protein with a deleted RING domain (Figure S1C). These FP results further confirm the specific binding of XIAP IRES to the MDM2 RING domain, as previously noted (Gu et al., 2009; Liu et al., 2015).

In order to evaluate whether the FP assay was suitable for HTS application, we analyzed the signal-to-noise (S/N) ratios and Z′ factors of the assay. At a constant concentration of 1 ng/ml fluorescent RNA probe, both the S/N ratios and Z′ factors increased with increasing concentrations of MDM2 protein (Figure 1C). When the MDM2 concentration was increased above 40 μg/ml, the FP assay gave S/N ratio >8 and a Z′ factor above 0.5. These parameters indicate a robust assay performance suitable for HTS (Du et al., 2007).

Next, we performed HTS with the optimized FP assay in 4 chemical libraries containing a total of 141,394 known reagents, drugs and small-molecule compounds (Figures 1D–G). These screenings resulted in a total of 426 hits based on decreased assay “window” of more than 50–70%. Dose-response assays (Figure S1D) were then carried out with each of these 426 candidate compounds to determine the concentration needed for achieving 50% inhibition (IC50). This resulted in identification of 95 compounds with an IC50 of less than 25 μM.

Identification of inhibitors targeting MDM2 and XIAP expression in cancer cells

We performed Western blot assays in cancer cells treated with the above 95 compounds (labeled MX1-95). For this, we used cell lines from two tumor types, acute lymphoblastic leukemia (ALL) and neuroblastoma (NB). We found that 8 of the 95 compounds clearly inhibited the expression of both MDM2 and XIAP proteins (Figures 2A, B and S2). Further examination of three selected compounds (MX3, MX11 and MX69) showed that they inhibited expression of both MDM2 and XIAP in a time- and dose-dependent manner (Figures 2C–E). As controls, we established that these compounds did not change the levels of Bcl-2, cIAP-1 and cIAP-2 protein expression, suggesting that they specifically inhibit MDM2 and XIAP.

Characterization of leads binding to either MDM2 RING protein or XIAP IRES

We performed binding assays to determine whether the selected lead compounds (leads) bind to either MDM2 RING protein or to XIAP IRES to block their interaction. The GST-MDM2 RING protein has natural fluorescence with excitation of 280 nm and emission of 335 nm (Figure 3A). XIAP IRES labeled with fluorescence has an excitation of 485 nm and emission of 530 nm (Figure S3A). We performed fluorescent titration assays to determine binding of each of the 8 leads to MDM2 RING protein (Figure 3B) and XIAP IRES (Figure 3C). Five leads (MX5, MX11, MX61, MX69 and MX92) were able to bind to MDM2 RING protein with binding K_d values of 3.78, 5.21, 3.72, 2.34 and 4.56 μM, respectively (Figure 3D). None of the 5 MDM2-binding leads bound to XIAP IRES (Figures 3E and S3B). In contrast, two leads (MX3 and MX25) bound to XIAP IRES with binding K_d of 5.26 and 10.48 uM, respectively (Figure 3E); neither of these leads bound to MDM2 RING protein

(Figures 3D and S3C). MX6 bound neither to MDM2 RING protein nor to XIAP IRES. As controls, the selected leads did not bind either to the GST protein or to an XIAP non-IRES probe (Figures S3D and E).

We also performed ITC assays to confirm binding of MX69 to MDM2 RING protein and MX3 to XIAP IRES, respectively. Consistent with the fluorescent titration results, MX69 (but not MX3) bound to the MDM2 RING protein with a binding K_d of 2.75 uM (Figures 3F and G), whereas MX3 (but not MX69) bound to XIAP IRES with a binding K_d of 5.83 (Figures S3F and G).

Selected leads induce MDM2 self-ubiquitination and degradation

We previously demonstrated that binding of XIAP IRES to the MDM2 RING domain decreased MDM2 self-ubiquitination and degradation (Liu et al., 2015). We further tested whether our selected leads, which block the XIAP IRES-MDM2 RING domain interaction, were able to reverse the XIAP IRES-mediated decrease in MDM2 self-ubiquitination and degradation. Before testing this possibility, we performed a UV cross-linking and RNA-protein binding assay to confirm the effect on the interaction between XIAP IRES and MDM2 RING protein. As expected, all 8 leads disrupted the interaction between XIAP IRES RNA and MDM2 RING protein (Figure 4A). Furthermore, co-transfection and in vivo ubiquitination assays showed that all 8 leads reversed XIAP IRES-mediated inhibition of MDM2 self-ubiquitination (Figure 4B).

We selected MX3 and MX69, which show good binding to XIAP IRES and to MDM2 protein respectively, to determine their effects on MDM2 ubiquitination and protein level. IP-Western blot assay showed that both MX3 and MX69 induced ubiquitination of endogenous MDM2 in cancer cells (Figures 4C and S4A). MX69-mediated downregulation of MDM2 protein was inhibited by protein-degradation inhibitor MG132 (Figure 4D). This suggests that downregulation of MDM2 by MX69 is through a protein-degradation mechanism. CHX pulse-chase assay confirmed that the half-life of MDM2 in control-treated EU-1 cells was greater than 90 min, whereas MX69 treatment decreased MDM2 half-life to < 30 min (Figure 4E), further suggesting that MX69 induces MDM2 degradation.

In experiments utilizing NB cells, SK-N-SH cells were stably transfected with either WT-MDM2 or mutant MDM2-C464A, a form lacking ubiquitin activity. Treatment with MX69 significantly inhibited expression and increased turnover of WT-MDM2 but not MDM2-C464A (Figures 4F, G and S4B) in plasmid-transfected SK-N-SH cells. These results further suggest that MX69 downregulates MDM2 through induction of MDM2 self-ubiquitination and degradation.

Downregulation of MDM2 results in activation of p53 and inhibition of XIAP

Since p53 is an important inhibitory target of MDM2, we evaluated the expression and function of p53 following lead-mediated downregulation of MDM2. First, we evaluated the effect of MX69 on expression and turnover of p53 protein in the MDM2-overexpressing/WT-p53 cell line EU-1. Results from pulse-chase experiments showed that p53 half-life in control-treated cells was less than 30 min, while it was remarkably increased

by MX69 (Figure 4E). Similarly, MX69 significantly enhanced p53 half-life in WT-MDM2 but not mutant MDM2-C464A transfected SK-N-SH cells (Figure 4G and S4B).

These results suggest that p53 is stabilized and accumulates in MX69-treated cells. Western blot results from EU-1 cells treated with MX3 or MX69 confirmed that p53 protein levels were significantly increased 2 to 8 hr after treatment (Figure 5A). Consistent with increased p53 protein expression, its transcriptional targets p21 and PUMA were also upregulated, resulting in G1 cell-cycle arrest (Figures 5B, left, 5C and S5A, left). In contrast, G1 cell-cycle arrest did not occur in MX69-treated EU-1 cells in the presence of sip53 (Figure 5B, right). Similarly, MX3 failed to induce G1 arrest in p53-mutant EU-6 (Figure S5A, middle) and p53-null EU-8 cells (Figure S5A, right); instead, a significant G2/M arrest was detected in the MX3-treated p53-mutant EU-6 cells (Figure S5A, middle).

The results in Figure 2 show that the selected leads also inhibited expression of XIAP. We evaluated whether inhibition of XIAP is associated with downregulation of MDM2. We used CRISPR/Cas9 to mutate MDM2 in SH-EP1 cells and then treated these MDM2 silenced cells with MX69. MX69 inhibited XIAP in control SH-EP1 cells but not in SH-EP1 with MDM2 KO (Figure 5D), suggesting that MX69-mediated inhibition of XIAP is MDM2-dependent.

In addition, we investigated whether MX69-mediated inhibition of XIAP occurred at the translational level. We performed linear sucrose-gradient fractionation to assess the state of polyribosome association of XIAP mRNA in EU-1 cells subjected to either MX69 or control MX68 treatment (Figure S5B). We found that MX69 induced a downregulation in polyribosome association. This was shown by a shift in XIAP mRNA from fractions containing enriched translating polyribosomes to fractions containing translation-inactive complexes (Figure 5E). Furthermore, we evaluated whether MX69 inhibits XIAP translation through an IRES-dependent mechanism. Using gene transfection and reporter assays with the dicistronic plasmid pRL-xi-FL, we found that MX69 inhibited XIAP IRES-mediated translation of firefly luciferase (FL) (Figure S5C). As control, no activity of MX69 on the MYCN IRES was detected (Figure S5D). Figures S5E and F show no alteration of FL mRNA in transfection of dicistronic reporter plasmids with insertion of the XIAP or MYCN IRES, suggesting that these IRES regulated FL activity occurs solely at the translational level. MX69 did not regulate either XIAP transcription or its mRNA and protein stability (Figures S5G, H and 4E).

Finally, we performed Western blot and ELISA assays to evaluate the effect of leads on activation of caspases 3, 7 and 9, as well as on cleavage of the death substrate PARP. As shown in Figures 5F and G, activation of these caspases and cleavage of PARP were detected after treatment with either MX3 or MX69.

Selected leads induce apoptosis and death in cancer cells

In order to evaluate the effects of selected leads on cancer-cell viability and apoptosis, we tested 12 cancer cell lines (6 ALL and 6 NB) with different MDM2 expression levels and p53 status, as summarized in Table S1. WST cytotoxicity assays showed that all 8 leads exhibited different cytotoxic activities against these cell lines, with MX3 having the most

potent cytotoxic effect (Table S1). MX69 also exhibited a significant cytotoxic effect on both ALL and NB lines, particularly those lines with MDM2 overexpression and a WT-p53 phenotype (Figure 6A and B). Figure 6C shows representative photomicrographs indicating cell growth inhibition and/or cell death in NB-1691 cells following treatment by MX69.

To clarify whether the observed cell death was associated with induction of apoptosis, we stained cells with Annexin-V FITC, and quantitated the results by flow cytometry and fluorescence microscopy. We found that MX69- and MX3-induced cell death was indeed due to apoptosis. As seen in Figure 6D, over 90% of cells were Annexin-V positive (green cells) in MX69-treated EU-1 cells. Flow cytometry showed that MX69 and MX3 induced apoptosis and cell death in both a time- (Figures 6D and S6A) and dose- (Figures 6E and S6B) dependent manner.

The effects of MX69 and MX3 on human normal bone marrow mononuclear (NBMM) cells were evaluated using the WST cytotoxic assay. These experiments showed over 90% cell survival of NBMM following treatment with MX69 at a dose of 2–8 μM for 24 hr. Similar treatment with MX3 showed that NBMM cell survival was only about 50% at a dose of 2 μM (Figure 6F).

In addition, we evaluated the effect of these compounds on normal human hematopoiesis using clonogenic analyses for CFU-GM and BFU-E. Results showed that MX69 at 10 μM had little inhibitory effect on CFU-GM and BFU-E. In contrast, MX3 at 1 μM showed severe inhibitory effects on CFU-GM and BFU-E. As seen in Figures 6G and H, in the MX69-treated samples the CFU-GM and BFU-E colony number and size were similar to the control, whereas both these parameters were significantly reduced in the MX3-treated samples.

MX69-induced cell apoptosis and death are dependent on MDM2, p53 and XIAP expression

We further tested whether cell apoptosis and death induced by selected leads can be attributed to high-level expression of MDM2 and XIAP as well as p53 activation. We performed KO or transfection of these factors in several selected cancer cell lines with different expression levels of MDM2 and p53 status and tested their response to MX69. We silenced MDM2 using the CRISPR/Cas9 genome editing approach in MDM2-overexpressing EU-1 and SH-EP1 cells. KO of MDM2 resulted in significant resistance of these cells to MX69 compared with non-MDM2-silenced (control) cells (Figure 7A). In contrast, SK-N-SH cells (expressing low endogenous levels of MDM2) exhibited a significantly increased cell death response to MX69 following stable transfection of MDM2 compared with control plasmid-transfected cells (Figure 7B). These results suggest that MX69-induced cell death is MDM2 dependent.

Since MDM2 is an inhibitor of p53, we tested whether activation of p53 plays a role in MX69-induced cancer cell death following inhibition of MDM2. We used sip53 to silence p53 in both MDM2-overexpressing (naturally or enforced) and non-MDM2-overexpressing (naturally or KO) cells that were treated with MX69. We found that silencing p53 significantly inhibited MX69 activity in MDM2-overexpressing EU-1 and SH-EP1 as well as MDM2-transfected SK-N-SH; in contrast, silencing p53 did not significantly inhibit

MX69 activity in non-MDM2-overexpressing SK-N-SH and MDM2-KO EU-1 and SH-EP1 (Figures 7A, B and S7A). These results suggest that MX69-induced cell death involves inhibition of MDM2 and consequent upregulation of p53 activity. In addition, SK-N-SH cells transfected with mutant MDM2-C464A were less sensitive to MX69, and MX69-induced cell death was not inhibited by sip53 (Figure. 7B), further suggesting that MX69 induces cell death not only by decreasing MDM2 protein levels but also by inhibiting MDM2 E3 ligase activity for p53. Furthermore, we found that p53 activity in NBMM cells (which express very low levels of MDM2) was significantly induced by MX3 but not by MX69 (Figure S7B).

We also tested the role of XIAP, which is regulated by MDM2 in MX69-induced cancer cell death. We first selected a p53-null NB cell line (LA1-55N) that was transfected with MDM2. Inhibition of XIAP by siRNA decreased sensitivity of the MDM2-transfected LA1-55N to MX69 (Figure 7C). Similarly, inhibition of XIAP reduced sensitivity to MX69 of WT-p53/MDM2 overexpressing NB-1691 cells (Figure 7D). In contrast, inhibition of XIAP increased sensitivity of these cells to doxorubicin (Figure S7C). This suggests that XIAP expression specifically contributes to MX69-induced apoptosis, and that depletion of XIAP has an additive role in cell death induced by commonly used genotoxic drugs such as doxorubicin, indicating that XIAP is not a target of doxorubicin.

We also performed double-KO of both MDM2 and XIAP using siRNA, and then, treated the cells with MX69 in NB-1691 cells. Results as shown in Figures 7D indicated that simultaneous inhibition of both MDM2 and XIAP resulted in greater resistance to MX69-induced apoptosis as compared to KO of each factor alone. We tested the expression levels of MDM2, XIAP and p53 in cells treated with MX69, KO of MDM2 and/or XIAP or their combinations. We found that significant induction of p53 was detected in cells treated with MX69 alone following rapid degradation of MDM2 at 8–24 hr (Figures S7D and E). In contrast, p53 was not significantly induced by siMDM2, although a significant reduction of MDM2 was detected at 48 hr post transfection of siMDM2 (Figure S7E). Induction of p53 was also not detected in cells with combination of MDM2/XIAP KO and MX69. The p53 induction in MX69-treated cells was consistent with the apoptosis results as shown in Figure 7D, further suggesting the importance of p53 activation in induction of apoptosis by MX69.

Similarly, double-KO of p53 and XIAP resulted in much greater resistance to MX69 as compared to KO of p53 or XIAP alone (Figure S7F) suggesting that both MDM2 and XIAP are targets of MX69 and that XIAP inhibition and p53 activation due to MDM2 degradation contribute to the apoptotic activity of MX69.

MX69 inhibits cancer progression in vivo

Since MX69 significantly inhibited tumor but not normal cells in vitro, we evaluated its anti-cancer activity in vivo, using an animal model. First, we determined the maximum tolerated dose (MTD) of MX69 in order to define the appropriate in vivo dosage. MX69 doses at 25, 50, 100, 200 and 400 mg/kg were given i.p. to Hsd:ICR (CD-1) normal mice (6 mice per group), at 24 hr intervals for a period of 3 days (1 course). After a 4-day rest, this dosage schedule was repeated for a second course. The 400 mg/kg dose was lethal within 20 days

for two out of six mice, whereas doses between 25 and 200 mg/kg were well tolerated, with no deaths by day 30 (Figure S8A).

To test whether MX69 has antitumor activity in vivo, we administered MX69 to SCID mice previously inoculated with EU-1 leukemia cells. Using dose levels established in vitro, we treated mice (10 mice per group) with 3 doses of MX69 (50, 75 and 100 mg/kg), using the same schedule as for the MTD test. Our results showed that control mice experienced significant loss of body weight and changes in fur pattern (either piloerection or matted fur) within 30–40 days after EU-1 inoculation, while the MX69-treated mice showed no adverse effects at up to 40-days post-treatment (Figures 8A and S8B). All untreated control SCID mice died within 45 days after inoculation, while all mice treated with 100 mg/kg MX69 still survived after 150 days. Forty percent of the 50 mg/kg MX69-treated mice died within the 98–143 days after inoculation, as did 20 percent of the 75 mg/kg MX69-treated mice (Figure 8B).

All control mice injected with EU-1 cells died within 45 days, suggesting successful engraftment of human EU-1 cells. To further confirm this, we examined them for presence of EU-1 blasts in the peripheral blood. All control mice showed evidence of progressive leukemia. Histological analysis showed presence of human ALL blasts in peripheral blood of control but not MX69-treated mice (Figure 8C). Similarly, PCR analysis showed presence of human β-globin gene in control but not MX69-treated mice (Figure 8D).

In addition to the MTD test, we evaluated the possible toxic effects of MX69 in vivo. We treated the Hsd:ICR (CD-1) normal mice with MX69 at doses of 50, 75 and 100 mg/kg, using the same schedule as for the MTD test. Histopathological analysis of harvested heart, liver and kidney tissue showed no evidence of toxicity after treatment with MX69 at the 100 mg/kg dose (Figure 8E). In contrast, MX3 treatment at a much lower dose (20 mg/kg) led to pronounced heart tissue damage, with increased cytoplasmic vacuolization and myofibrillar loss (Figure 8E, upper right). Hematological tests showed no significant decreases in WBC and PLT; furthermore, there were no significant increases in ALT, AST and BUN in 100 mg/kg MX69-treated mice (Figures 8F, G and S8C-E). In contrast, significantly decreased WBC and increased ALT were detected in mice treated with MX3 at 20 mg/kg dose (Figure 8H and I).

DISCUSSION

MDM2 and XIAP proteins are important cell-survival factors in tumor cells. The major oncogenic function of MDM2 is promotion of cancer progression via inhibition of the p53 tumor suppressor, while XIAP acts as an anti-apoptotic protein playing a critical role in development of anticancer resistance through inhibition of caspases-mediated apoptosis. MDM2 gene amplification or protein overexpression has been detected in a variety of human cancers (Bueso-Ramos et al., 1993; Momand et al., 1998). MDM2 overexpression is associated with disease progression and poor treatment outcome (Nakayama et al., 1995; Polsky et al., 2002; Teoh et al., 1997; Zhou et al., 2000). Similarly, upregulated XIAP is detected in many cancer patients, and a high level of XIAP expression is associated with resistance to chemotherapy and poor prognosis (Berezovskaya et al., 2005; Mizutani et al.,

2007; Tamm et al., 2004). Efforts have been made to target the XIAP-caspase and MDM2-p53 interactions or MDM2 E3 ligase activity as therapeutic strategies (Huang et al., 2004; Rajapakse, 2007; Ray-Coquard et al., 2012; Shangary et al., 2008; Vassilev et al., 2004; Wade et al., 2013; Yang et al., 2005). Moreover, it has been demonstrated that concomitant inhibition of both MDM2 (by the MDM2-p53 inhibitor nutlin-3a) and of XIAP (by small molecule antagonists) synergistically induced apoptosis in WT-p53 leukemia cells (Carter et al., 2010).

Although targeting either MDM2-p53 interaction or MDM2 E3 ligase activity can induce p53 and cancer cell apoptosis, a limiting factor is that targeting these mediators has beneficial cytotoxic and apoptotic effects only in cancer cells bearing normal p53; tumor cells with mutant p53 are not inhibited. In addition, none of these inhibitors block MDM2 expression. To the contrary, MDM2 expression can be enhanced by activated p53 via induction of MDM2 promoter activity (Juven et al., 1993) or by increased MDM2 protein stabilization (Yang et al., 2005). Augmented MDM2 can inhibit apoptosis via p53-independent roles such as induction of XIAP, which could counteract the apoptotic activity of inhibitors like nutlin-3 and HLI98. Furthermore, MDM2-p53 interaction inhibitors (e.g. the nutlin-related clinical candidate RG7112) can induce activation of p53 in the hematopoietic system, resulting in hematological toxicities such as neutropenia and thrombocytopenia (Iancu-Rubin et al., 2014; Ray-Coquard et al., 2012).

Several studies have focused on compounds that specifically downregulate MDM2 expression (Qin et al., 2012). These agents have been found to inhibit MDM2 expression through different mechanisms. For example, the dietary component curcumin downregulates MDM2 via the PI3K/mTOR/ETS2 pathway (Li et al., 2007); the natural product berberine can induce MDM2 degradation through disrupting the MDM2-DAXX-HAUSP interaction (Zhang et al., 2010); and the natural product triptolide inhibits MDM2 expression by suppressing MDM2 mRNA synthesis (Huang et al., 2013; Wang et al., 2014a). In addition, a small-molecule compound (SP-141) was recently identified that binds to the N-terminus of MDM2 and induces MDM2 protein degradation. However, the exact mechanism by which SP-141 causes MDM2 degradation remains largely unknown (Wang et al., 2014b).

The present study used FP-HTS to identify inhibitors targeting the MDM2 C-terminal RING protein-XIAP IRES interaction. The goal was to select for molecules that inhibit MDM2 as well as XIAP expression in cancer cells. Our FP-HTS studies identified eight compounds that showed inhibitory effects on MDM2 and XIAP. These MDM2/XIAP inhibitors are mainly divided into two classes: one that binds to XIAP IRES RNA, and one that binds to the MDM2 RING protein. Both classes of inhibitor block MDM2-XIAP RNA interaction, resulting in MDM2 self-ubiquitination and degradation as well as repression of XIAP translation. Furthermore, we found that their cytotoxic and anti-proliferative effects are due to their ability to both inhibit XIAP expression and induce p53 activity by blocking MDM2.

With regard to XIAP RNA-binding agents, we cannot rule out possible off-target effects these compounds may have in inducing apoptosis due to interaction with other cellular RNA molecules or activation of other signaling pathways. These RNA-binding compounds may also show significant toxicity to normal cells. In fact, our experimental results demonstrated

that the XIAP RNA-binding MX3 (subsequently identified as the chemotherapeutic drug mitoxantrone, which binds to numerous RNA and DNA molecules (Durr et al., 1983; Riahi et al., 2008; Zheng et al., 2009), had a strong inhibitory effect on normal human hematopoiesis and induced tissue damage in animal studies, although the toxicity could also come from other activities of this drug. Nevertheless, XIAP RNA-binding compounds may have limited clinical use.

In contrast to XIAP RNA-binding agents, MDM2 protein-binding inhibitors may have significant clinical potential since cancer cells (unlike normal cells) often express high levels of MDM2. Specifically, we found that the MDM2-binding compound MX69 has significant apoptotic and anti-proliferative effects on MDM2-expressing cancer cells both in vitro and in vivo. Furthermore, unlike the RNA-binding agent mitoxantrone, MX69 shows minimal inhibitory effect on normal human BM in vitro and is well tolerated in animals due to the fact that normal cells/tissues express little or no MDM2. This suggests that MDM2-specific agent MX69 should not activate either on-target (e.g. p53 induction) or off-target signaling pathways in normal cells. Thus, specific MDM2 inhibitors such as MX69 may be excellent candidates for targeted therapy of refractory cancers expressing high levels of MDM2.

We believe development of MDM2/XIAP inhibitors as potential anticancer drugs represents a strategy for improving cancer outcome, since they may suppress or kill cancer cells much more potently than MDM2-p53 inhibitors: In WT-p53 cancer cells, treatment with a drug that simultaneously inhibits MDM2 and XIAP should result not only in the activation of p53, but also in induction of caspases 3, 7 and 9. Additionally, these inhibitors should be capable of inducing apoptosis in p53-deficient cancer cells expressing both MDM2 and XIAP.

EXPERIMENTAL PROCEDURES

Cells

This study used six ALL cell lines (EU-1, EU-3, EU-6 and EU-8, SUP-B13 and UOC-B1) and six NB cell lines (NB-1691, NB-1643, SH-EP1, IMR-32, SK-N-SH and LA1-55N). All 12 cancer cell lines were established from pediatric ALL or NB patients and were well-characterized for their expression of MDM2 and p53-status (Table S1), as reported previously (Gu et al., 2012; He et al., 2011; Zhou et al., 1995). The 293T cell line was used for gene transfection and in vivo ubiquitination assays. Approved by the Emory University Institutional Review Board (IRB), human normal bone marrow mononuclear (NBMM) cells were obtained from five donors after informed consent, and were used for clonogenic assays to measure the effect of selected leads on normal hematopoiesis.

Plasmids and transfection

The MDM2 expression plasmids were generated by PCR and cloned into a pCMV expression vector. Site-directed mutagenesis (Quick Change Mutagenesis Kit, Stratagene) was used to mutate MDM2 at 464 (Cys to Ala), thus generating MDM2-C464A plasmid. The GST-tagged MDM2 and MDM2 RING domain constructs were cloned into the bacterial pGEX expression vector. The XIAP IRES RNA expression plasmid was generated by

cloning an RNA fragment containing the XIAP IRES region into the pRNA-CMV3.1-puro vector. The XIAP expression plasmid was provided by Dr. Lily Yang (Emory University). The pCI-His-hUbi plasmid was purchased from Addgene. Transfections were performed using Lipofectamine™ 2000 reagents (Invitrogen).

Fluorescence polarization assay and chemical screening

The MDM2 RING protein and the XIAP IRES probe were synthesized and labeled as described in the supplemental information. An FP assay to monitor the interaction of MDM2 RING protein with XIAP IRES was carried out in black 1536-well microplates, in a total volume of 4.6 μL per well. First, assay reaction buffer (40 μg/ml MDM2 RING protein and 1 ng/ml XIAP IRES probe in Hepes buffer; total 4.5 μL) was dispensed into each well. Then the test compound (0.1 μL of 1 mM stock in DMSO) was added to the reaction buffer, using pintool integrated with BeckmanNX (Beckman Coulter) for a final compound concentration of 21.7 μM. For each assay plate, the following controls were included: 32 wells with XIAP IRES only and 32 wells with a combination of MDM2, XIAP IRES and DMSO alone. Plates were incubated at room temperature for 2 hr and FP values (in millipolarization (mP) units) were measured with an Envision multi-label plate reader (PerkinElmer). An excitation filter at 480/30 nm and two emission filters (FP P-pol 535/40 and FP S-pol 535/40) were used with a dual mirror of D505fp/D535 nm. Data analysis was conducted using CambridgeSoft software. The activity cutoff was set as a percentage inhibition greater than 50–70%. Additionally, fluorescence intensity (FI) value of vehicle control at <1.5–2.

Compound-protein and compound-RNA binding assays

The binding activity of selected leads to either MDM2 protein or XIAP IRES was examined by fluorescence titration and isothermal titration calorimetry (ITC) assays, as described in detail in Supplemental Experimental Procedures online.

Immunoprecipitation and Western blot assay

Cells were lysed in a buffer composed of 50 mM Tris, pH 7.6, 150 mM NaCl, 1% Nonidet P-40, 10 mM sodium phosphate, 10 mM NaF, 1 mM sodium orthovanadate, 2 mM phenylmethylsulfonyl fluoride (PMSF), 10 μg/ml aprotinin, 10 μg/ml leupeptin and 10 μg/ml pepstatin. After centrifugation, the clarified cell lysate was separated from the pellet of cell debris and incubated with Protein G plus/Protein A-agarose and antibodies. For the Western blot, the resulting cell lysates or immunoprecipitates were resolved by SDS-PAGE. They were then transferred to a nitrocellulose filter and probed with the specific antibodies. Finally, proteins were visualized with a chemiluminescent detection system (Pierce).

Ubiquitination assay

Ubiquitination assay was performed as described previously (Pan and Chen, 2003). Briefly, gene transfected cells were treated with or without selected reagents and MG132, and then collected in two aliquots. One aliquot (10%) was used for conventional Western blotting. The remaining cells (90%) were used for the purification of His6-tagged protein, with the aid of Ni^{2+}-nitrilotriacetic acid beads. Purified His-tagged protein was then eluted and analyzed by Western blot assay.

Cytotoxicity assay

The cytotoxic effect of leads was determined using the water-soluble tetrazolium salt (WST) assay. Briefly, cells cultured in 96-well microtiter plates were treated with different concentrations of leads for a 20-hr period. WST (25 μg/well) was then added and incubation continued for an additional 4 hr, after which optical density (OD) was read with a microplate reader (test wavelength of 450 nm; reference wavelength of 620 nm).

Flow cytometry

Flow cytometry was performed to analyze cell-cycle position and state of apoptosis. For cell-cycle analysis, cells were collected, rinsed and fixed in 70% ethanol, and then washed again and re-suspended in PBS solution containing propidium iodide. The samples were analyzed using a FACScan. For quantitative detection of apoptosis, cells with or without treatment were washed with PBS and stained with FITC-annexin V and 7-AAD using a FITC Annexin V Apoptosis Detection Kit 1 (BD Pharmingen™) following manufacture's instruction and analyzed by flow cytometry.

Animal studies

Animals were housed, maintained, and treated at Emory University Children Center in accordance with protocols approved by the IACUC at Emory University. For the leukemic xenograft assay, the human ALL cell line EU-1 was engrafted into SCID mice. Cells (10^7 cells/mouse) were injected into the tail vein of 5-week-old female SCID mice (C.B-17/IcrHsd-Prkdc^{scid}Lyst^{bg}). At the 72-hr time point after injection, xenograft cohorts (10 for each treatment groups) were administered either MX69 at dose levels of 50, 75 and 100 mg/kg, or control agent. Intraperitoneal (i.p.) injection was used at 24 hr intervals for a period of 3 days (one course). After a 4-day rest, this dosage schedule was repeated for a second course.

Xenograft recipients were euthanized upon occurrence of hind-limb paralysis and evaluated for the presence of human leukemic cells by histopathology. Alternatively, a DNA sequence in exon 1 of the human β-globin gene was detected by PCR analysis. The in vivo testing endpoint in this leukemia model is survival. We analyzed the probability of event-free survival (EFS) for all treatment and control groups, constructed EFS curves using the Kaplan-Meier product limit method, and determined the effects of treatment with different dosages of MX69 on the probability of EFS, using the log-rank test.

Statistical analysis

All data represent mean ± SD of three independent experiments. A two-tailed t-test was performed to compare the difference between two groups. A p value <0.05 is considered significantly different and $p>0.5$ is considered not significant.

Supplementary Material

Refer to Web version on PubMed Central for supplementary material.

Acknowledgments

This work was supported by R01 grants (CA180519, CA123490 and CA143107) to M.Z.; the Scholar award (79387GA) from Hyundai Hope on Wheels to M.Z.; research grants from CURE Childhood Cancer to M.Z and L.G; U01 grant (CA168449) to H.F.; and a National Natural Science Foundation of China grant (No.81472488) to S.Z. We thank J. Yang (Georgia State University) for fluorescent titration support, K.Y. Chiang (Emory University) for providing human NBMM cells, and H. Findley (Emory University) for editing the manuscript.

References

Berezovskaya O, Schimmer AD, Glinskii AB, Pinilla C, Hoffman RM, Reed JC, Glinsky GV. Increased expression of apoptosis inhibitor protein XIAP contributes to anoikis resistance of circulating human prostate cancer metastasis precursor cells. Cancer research. 2005; 65:2378–2386. [PubMed: 15781653]

Bueso-Ramos CE, Yang Y, deLeon E, McCown P, Stass SA, Albitar M. The human MDM-2 oncogene is overexpressed in leukemias. Blood. 1993; 82:2617–2623. [PubMed: 8219216]

Candeias MM, Malbert-Colas L, Powell DJ, Daskalogianni C, Maslon MM, Naski N, Bourougaa K, Calvo F, Fahraeus R. P53 mRNA controls p53 activity by managing Mdm2 functions. Nature cell biology. 2008; 10:1098–1105. [PubMed: 19160491]

Carter BZ, Mak DH, Schober WD, Koller E, Pinilla C, Vassilev LT, Reed JC, Andreeff M. Simultaneous activation of p53 and inhibition of XIAP enhance the activation of apoptosis signaling pathways in AML. Blood. 2010; 115:306–314. [PubMed: 19897582]

Du Y, Moulick K, Rodina A, Aguirre J, Felts S, Dingledine R, Fu H, Chiosis G. High-throughput screening fluorescence polarization assay for tumor-specific Hsp90. Journal of biomolecular screening. 2007; 12:915–924. [PubMed: 17942784]

Durr FE, Wallace RE, Citarella RV. Molecular and biochemical pharmacology of mitoxantrone. Cancer treatment reviews. 1983; 10(Suppl B):3–11.

Gu L, Zhang H, He J, Li J, Huang M, Zhou M. MDM2 regulates MYCN mRNA stabilization and translation in human neuroblastoma cells. Oncogene. 2012; 31:1342–1353. [PubMed: 21822304]

Gu L, Zhu N, Zhang H, Durden DL, Feng Y, Zhou M. Regulation of XIAP translation and induction by MDM2 following irradiation. Cancer cell. 2009; 15:363–375. [PubMed: 19411066]

Haupt Y, Maya R, Kazaz A, Oren M. Mdm2 promotes the rapid degradation of p53. Nature. 1997; 387:296–299. [PubMed: 9153395]

He J, Gu L, Zhang H, Zhou M. Crosstalk between MYCN and MDM2-p53 signal pathways regulates tumor cell growth and apoptosis in neuroblastoma. Cell Cycle. 2011; 10:2994–3002. [PubMed: 21862876]

Holcik M, Lefebvre C, Yeh C, Chow T, Korneluk RG. A new internal-ribosome-entry-site motif potentiates XIAP-mediated cytoprotection. Nature cell biology. 1999; 1:190–192. [PubMed: 10559907]

Huang M, Zhang H, Liu T, Tian D, Gu L, Zhou M. Triptolide inhibits MDM2 and induces apoptosis in acute lymphoblastic leukemia cells through a p53-independent pathway. Molecular cancer therapeutics. 2013; 12:184–194. [PubMed: 23243057]

Huang Y, Lu M, Wu H. Antagonizing XIAP-mediated caspase-3 inhibition. Achilles' heel of cancers? Cancer cell. 2004; 5:1–2. [PubMed: 14749118]

Iancu-Rubin C, Mosoyan G, Glenn K, Gordon RE, Nichols GL, Hoffman R. Activation of p53 by the MDM2 inhibitor RG7112 impairs thrombopoiesis. Experimental hematology. 2014; 42:137–145. e135. [PubMed: 24309210]

Jung CH, Kim J, Park JK, Hwang SG, Moon SK, Kim WJ, Um HD. Mdm2 increases cellular invasiveness by binding to and stabilizing the Slug mRNA. Cancer letters. 2013; 335:270–277. [PubMed: 23438693]

Juven T, Barak Y, Zauberman A, George DL, Oren M. Wild type p53 can mediate sequence-specific transactivation of an internal promoter within the mdm2 gene. Oncogene. 1993; 8:3411–3416. [PubMed: 8247544]

Lewis SM, Holcik M. IRES in distress: translational regulation of the inhibitor of apoptosis proteins XIAP and HIAP2 during cell stress. Cell death and differentiation. 2005; 12:547–553. [PubMed: 15818406]

Li M, Zhang Z, Hill DL, Wang H, Zhang R. Curcumin, a dietary component, has anticancer, chemosensitization, and radiosensitization effects by down-regulating the MDM2 oncogene through the PI3K/mTOR/ETS2 pathway. Cancer research. 2007; 67:1988–1996. [PubMed: 17332326]

Liu T, Zhang H, Xiong J, Yi S, Gu L, Zhou M. Inhibition of MDM2 homodimerization by XIAP IRES stabilizes MDM2, influencing cancer cell survival. Molecular cancer. 2015; 14:65. [PubMed: 25888903]

Mizutani Y, Nakanishi H, Li YN, Matsubara H, Yamamoto K, Sato N, Shiraishi T, Nakamura T, Mikami K, Okihara K, et al. Overexpression of XIAP expression in renal cell carcinoma predicts a worse prognosis. International journal of oncology. 2007; 30:919–925. [PubMed: 17332931]

Momand J, Jung D, Wilczynski S, Niland J. The MDM2 gene amplification database. Nucleic acids research. 1998; 26:3453–3459. [PubMed: 9671804]

Momand J, Zambetti GP, Olson DC, George D, Levine AJ. The mdm-2 oncogene product forms a complex with the p53 protein and inhibits p53-mediated transactivation. Cell. 1992; 69:1237–1245. [PubMed: 1535557]

Nakayama T, Toguchida J, Wadayama B, Kanoe H, Kotoura Y, Sasaki MS. MDM2 gene amplification in bone and soft-tissue tumors: association with tumor progression in differentiated adipose-tissue tumors. International journal of cancer Journal international du cancer. 1995; 64:342–346. [PubMed: 7591308]

Pan Y, Chen J. MDM2 promotes ubiquitination and degradation of MDMX. Molecular and cellular biology. 2003; 23:5113–5121. [PubMed: 12860999]

Polsky D, Melzer K, Hazan C, Panageas KS, Busam K, Drobnjak M, Kamino H, Spira JG, Kopf AW, Houghton A, et al. HDM2 protein overexpression and prognosis in primary malignant melanoma. Journal of the National Cancer Institute. 2002; 94:1803–1806. [PubMed: 12464652]

Qin JJ, Nag S, Voruganti S, Wang W, Zhang R. Natural product MDM2 inhibitors: anticancer activity and mechanisms of action. Current medicinal chemistry. 2012; 19:5705–5725. [PubMed: 22830335]

Rajapakse HA. Small molecule inhibitors of the XIAP protein-protein interaction. Current topics in medicinal chemistry. 2007; 7:966–971. [PubMed: 17508928]

Ray-Coquard I, Blay JY, Italiano A, Le Cesne A, Penel N, Zhi J, Heil F, Rueger R, Graves B, Ding M, et al. Effect of the MDM2 antagonist RG7112 on the P53 pathway in patients with MDM2-amplified, well-differentiated or dedifferentiated liposarcoma: an exploratory proof-of-mechanism study. The Lancet Oncology. 2012; 13:1133–1140. [PubMed: 23084521]

Riahi S, Reza Ganjali M, Dinarvand R, Karamdoust S, Bagherzadeh K, Norouzi P. A theoretical study on interactions between mitoxantrone as an anticancer drug and DNA: application in drug design. Chemical biology & drug design. 2008; 71:474–482. [PubMed: 18384527]

Schimmer AD. Inhibitor of apoptosis proteins: translating basic knowledge into clinical practice. Cancer research. 2004; 64:7183–7190. [PubMed: 15492230]

Shangary S, Qin D, McEachern D, Liu M, Miller RS, Qiu S, Nikolovska-Coleska Z, Ding K, Wang G, Chen J, et al. Temporal activation of p53 by a specific MDM2 inhibitor is selectively toxic to tumors and leads to complete tumor growth inhibition. Proceedings of the National Academy of Sciences of the United States of America. 2008; 105:3933–3938. [PubMed: 18316739]

Tamm I, Richter S, Oltersdorf D, Creutzig U, Harbott J, Scholz F, Karawajew L, Ludwig WD, Wuchter C. High expression levels of x-linked inhibitor of apoptosis protein and survivin correlate with poor overall survival in childhood de novo acute myeloid leukemia. Clinical cancer research: an official journal of the American Association for Cancer Research. 2004; 10:3737–3744. [PubMed: 15173080]

Teoh G, Urashima M, Ogata A, Chauhan D, DeCaprio JA, Treon SP, Schlossman RL, Anderson KC. MDM2 protein overexpression promotes proliferation and survival of multiple myeloma cells. Blood. 1997; 90:1982–1992. [PubMed: 9292533]

Vassilev LT, Vu BT, Graves B, Carvajal D, Podlaski F, Filipovic Z, Kong N, Kammlott U, Lukacs C, Klein C, et al. In vivo activation of the p53 pathway by small-molecule antagonists of MDM2. Science. 2004; 303:844–848. [PubMed: 14704432]

Wade M, Li YC, Wahl GM. MDM2, MDMX and p53 in oncogenesis and cancer therapy. Nature reviews Cancer. 2013; 13:83–96. [PubMed: 23303139]

Wang BY, Cao J, Chen JW, Liu QY. Triptolide induces apoptosis of gastric cancer cells via inhibiting the overexpression of MDM2. Med Oncol. 2014a; 31:270. [PubMed: 25280518]

Wang W, Qin JJ, Voruganti S, Srivenugopal KS, Nag S, Patil S, Sharma H, Wang MH, Wang H, Buolamwini JK, Zhang R. The pyrido[b]indole MDM2 inhibitor SP-141 exerts potent therapeutic effects in breast cancer models. Nature communications. 2014b; 5:5086.

Yang Y, Ludwig RL, Jensen JP, Pierre SA, Medaglia MV, Davydov IV, Safiran YJ, Oberoi P, Kenten JH, Phillips AC, et al. Small molecule inhibitors of HDM2 ubiquitin ligase activity stabilize and activate p53 in cells. Cancer cell. 2005; 7:547–559. [PubMed: 15950904]

Zhang X, Gu L, Li J, Shah N, He J, Yang L, Hu Q, Zhou M. Degradation of MDM2 by the interaction between berberine and DAXX leads to potent apoptosis in MDM2-overexpressing cancer cells. Cancer research. 2010; 70:9895–9904. [PubMed: 20935220]

Zheng S, Chen Y, Donahue CP, Wolfe MS, Varani G. Structural basis for stabilization of the tau pre-mRNA splicing regulatory element by novantrone (mitoxantrone). Chemistry & biology. 2009; 16:557–566. [PubMed: 19477420]

Zhou M, Gu L, Abshire TC, Homans A, Billett AL, Yeager AM, Findley HW. Incidence and prognostic significance of MDM2 oncoprotein overexpression in relapsed childhood acute lymphoblastic leukemia. Leukemia. 2000; 14:61–67. [PubMed: 10637478]

Zhou M, Yeager AM, Smith SD, Findley HW. Overexpression of the MDM2 gene by childhood acute lymphoblastic leukemia cells expressing the wild-type p53 gene. Blood. 1995; 85:1608–1614. [PubMed: 7888679]

Zhou S, Gu L, He J, Zhang H, Zhou M. MDM2 regulates vascular endothelial growth factor mRNA stabilization in hypoxia. Molecular and cellular biology. 2011; 31:4928–4937. [PubMed: 21986500]

SIGNIFICANCE

MDM2 and XIAP are important cell-survival proteins in tumor cells. MDM2 acts as an oncoprotein, promoting cancer progression mainly through inhibition of the tumor suppressor p53, while the anti-apoptotic protein XIAP plays a critical role in development of resistance to treatment via inhibition of therapy-induced apoptosis. MDM2 overexpression and upregulated XIAP have been detected in various human cancers, and elevated MDM2 and XIAP expression in tumor cells is associated with disease progression and poor treatment outcome. Our studies have identified inhibitors that simultaneously target MDM2 and XIAP expression, contributing to cancer cell apoptosis and death. These dual MDM2/XIAP inhibitors may represent a class of apoptosis-inducing agents that could be developed as targeted drugs for cancer treatment.

Highlights

- MDM2/XIAP inhibitors are selected by FP-HTS via blocking MDM2-XIAP IRES interaction
- MDM2/XIAP inhibitors degrade MDM2, activate p53 and inhibit XIAP expression
- MDM2/XIAP inhibitors exibit anticancer activity in vitro and in animal models
- One of the MDM2/XIAP inhibitors MX69 is very well tolerated in animals

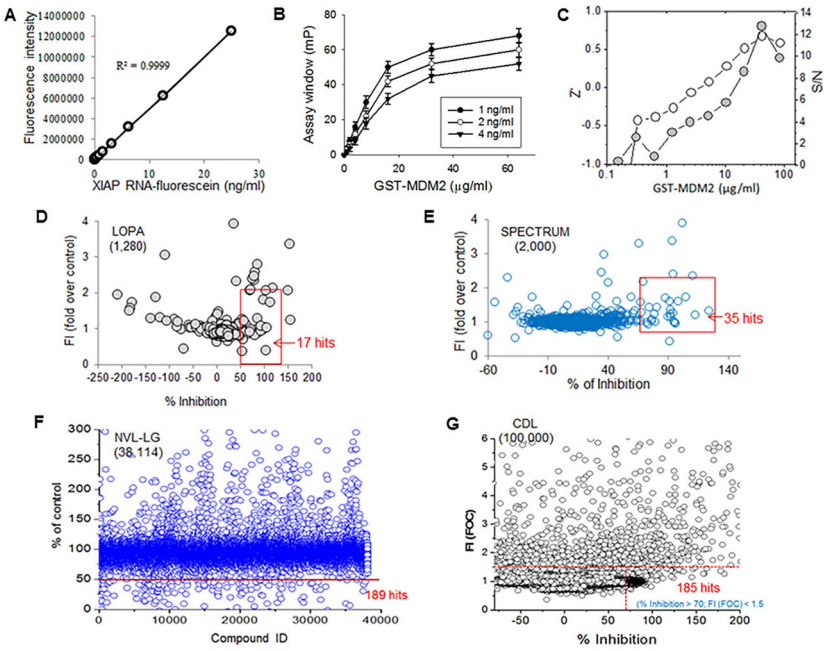

Figure 1.

Establishment and optimization of FP-HTS assay for selection of reagents and small-molecule compounds targeting MDM2 protein-XIAP IRES interaction (A) Detection of fluorescence for XIAP IRES RNA labeled with fluorescein. (B) FP assay for interaction between fluorescence-labeled XIAP IRES and MDM2 RING protein, data represent mean ± SD of three independent experiments. (C) Signal-to-noise (S/N) ratios and Z′ factors of the assay were obtained for estimating suitability of FP assay used for HTS. (D–G) HTS using optimized FP assay in four libraries, as indicated. The mP values for each well containing library agent were recorded. Percentage of inhibition was calculated to identify hits, as indicated on graph for each library, by setting activity cutoff at 50–70% inhibition and fluorescence intensity (FI) value of vehicle control at <1.5–2. See also Figure S1.

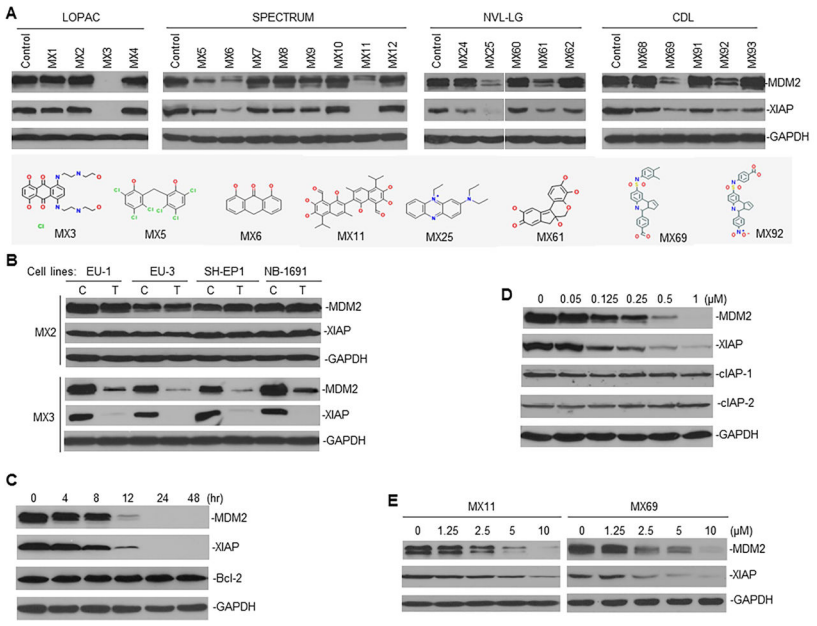

Figure 2.

Cell-based assay to select lead compounds (leads) inhibiting MDM2 and XIAP expression in cancer cells (A) Representative Western blots show MDM2 and XIAP expression in EU-1 ALL cells, when treated for 24 hr with promising hits selected from libraries as indicated. Dose of each hit used for cell treatment was equal to the IC50 value for fluorescence inhibition in HTS (data not shown). Structures of 8 leads inhibiting both MDM2 and XIAP were shown. (B) Western blot for MDM2 and XIAP expression in ALL (EU-1 and EU-3) and NB (SH-EP1 and NB-1691) cell lines having MDM2 overexpression, C, control; T, treatment. (C and D) Western blot for time-course (C) and dose-response (D) of MDM2 and XIAP inhibition in EU-1 cells treated with MX3 using indicated conditions. (E) Similar Western blot assays for MDM2 and XIAP expression in EU-1 cells treated with two additional leads (MX11 and MX69). See also Figure S2.

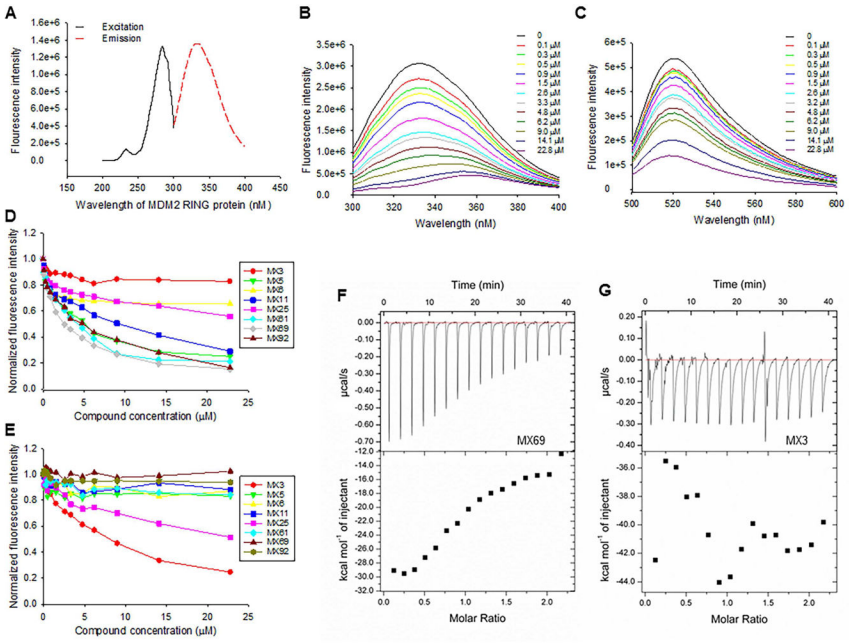

Figure 3.

Determination of selected leads binding to MDM2 RING protein or XIAP IRES RNA (A) Excitation and emission spectra of the GST-MDM2 RING protein. (B and C) Representative graphs showing fluorescence changes when MDM2 RING protein was titrated with MX69 (B) and XIAP IRES was titrated with MX3 (C). (D and E) MDM2 RING protein (D) and XIAP IRES (E) were subject to titration with increasing concentrations of all eight leads as indicated. Relative changes in fluorescence intensity were traced, as in (B) and (C), and normalized to derive a binding K_d. (F and G) Confirmation of binding between MDM2 RING protein and MX69 (F) and non-binding between MDM2 RING protein and MX3 (G) as detected by ITC. All experiments were performed at least three times. See also Figure S3.

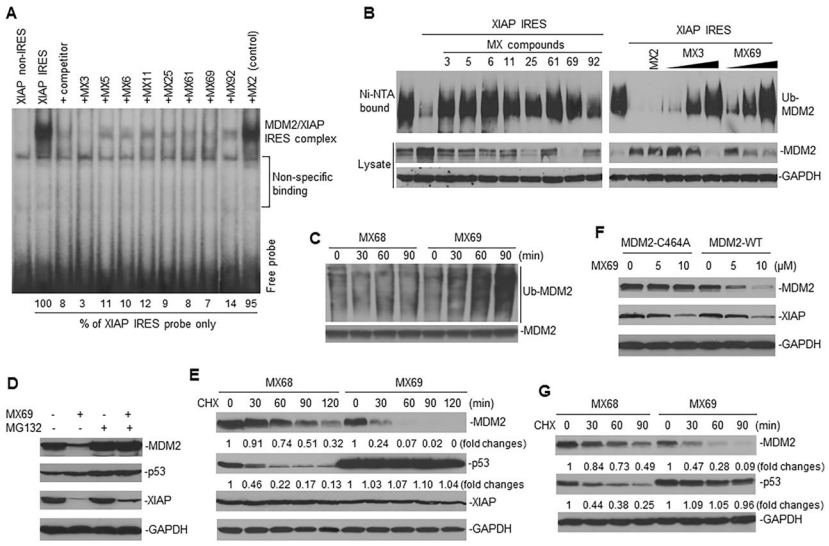

Figure 4.

Effect of leads on MDM2 self-ubiquitination and protein stability (A) UV cross-linking and RNA binding assay for testing effects of leads on the interaction between XIAP IRES (labeled with ^{32}P) and MDM2 protein. Controls include MX2 (no MDM2 inhibition), an XIAP non-IRES probe and 25-fold molar excess of unlabeled XIAP IRES (competitor). (B) Ubiquitination assay in 293T cells for testing effect of leads on self-ubiquitination of transfected MDM2 in presence or absence of XIAP IRES. Effects of either 1 μM of MX3 or 10 μM of other 7 leads are shown (left panel); right panel shows effects of increasing concentrations of either MX3 (0.25, 0.5 and 1 μM) or MX69 (2.5, 5 and 10 μM). (C) IP and Western blot assay using anti-MDM2 and anti-ubiquitin antibodies respectively, to detect effects of MX69 (10 μM) on ubiquitination of endogenous MDM2 in EU-1 cells. MX68 served as control. (D) EU-1 cells with or without MX69 treatment (10 μM for 8 hr) were treated with 10 μM MG132 for additional 4 hr and protein expression then detected by Western blot. (E) Protein turnover in EU-1 cells treated with 10 μM MX69 and MX68 (control) for 4 hr, as detected by CHX pulse-chase assay. (F) SK-N-SH cells stably transfected either with MDM2-WT or MDM2-C464A were treated with different doses of MX69 as indicated for 24 hr; MDM2 and XIAP were detected by Western blot. (G) A similar CHX pulse-chase assay as in (E) for MDM2 and p53 protein turnover in SK-N-SH cells stably transfected with WT-MDM2 following treatment with MX69. See also Figure S4.

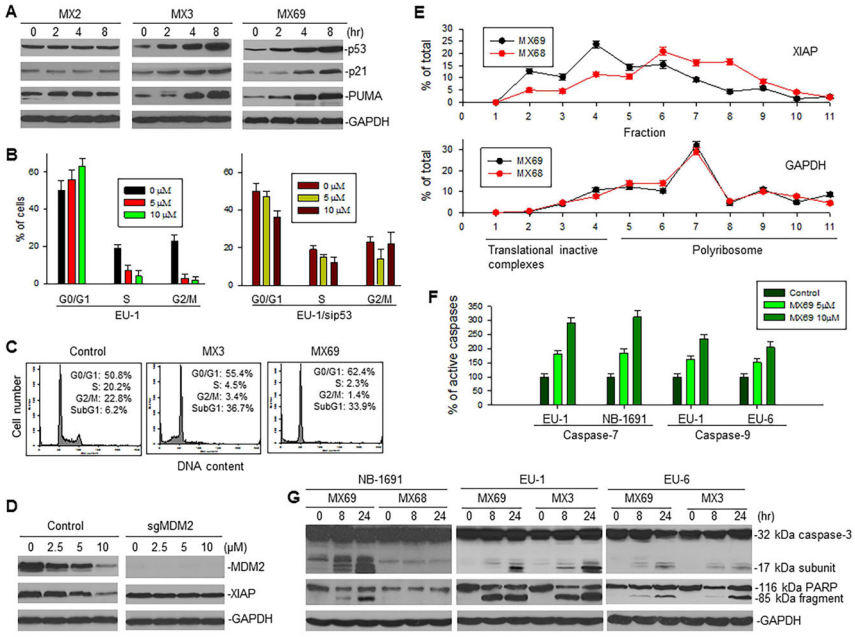

Figure 5.

Effect of leads on expression and function of p53 and XIAP following inhibition of MDM2 (A) Western blot for expression of p53 and its targets p21 and PUMA in EU-1 cells treated with 1 μM MX3 or 10 μM MX69 for indicated times. (B) Cell-cycle distribution of EU-1 and EU-1/sip53 cells treated with MX69 for 8 hr. (C) Representative flow cytometry histographs for EU-1 cells, both control and treated with 1 μM MX3 and 10 μM MX69. (D) Western blot for expression of MDM2 and XIAP in SH-EP1 cells with MDM2 KO by CRISPR/Cas9 (sgMDM2), treated with indicated doses of MX69 for 24 hr. (E) EU-1 cells were treated with either 10 μM MX69 or MX68 (control) for 4 hr and their cytoplasmic lysates were fractionated on a sucrose gradient. RNA was extracted from each of the fractions and subjected to qRT-PCR for analysis of the distribution of XIAP and GAPDH mRNAs. Data show the percentage of the total amount of corresponding mRNA in each fraction and represent mean ± SD of three independent experiments. (F) ELISA for activation of caspase-7 and -9 in ALL and NB cells treated with different doses of MX69 as indicated for 8 hr. (G) Western blot showing activation of caspase-3 and cleavage of death substrate PARP in cancer cells following treatment with 10 μM MX69 and MX68 (control) or 1 μM MX3 for times indicated. Data in (B and F) represent mean of three independent experiments, bars ± SD. See also Figure S5.

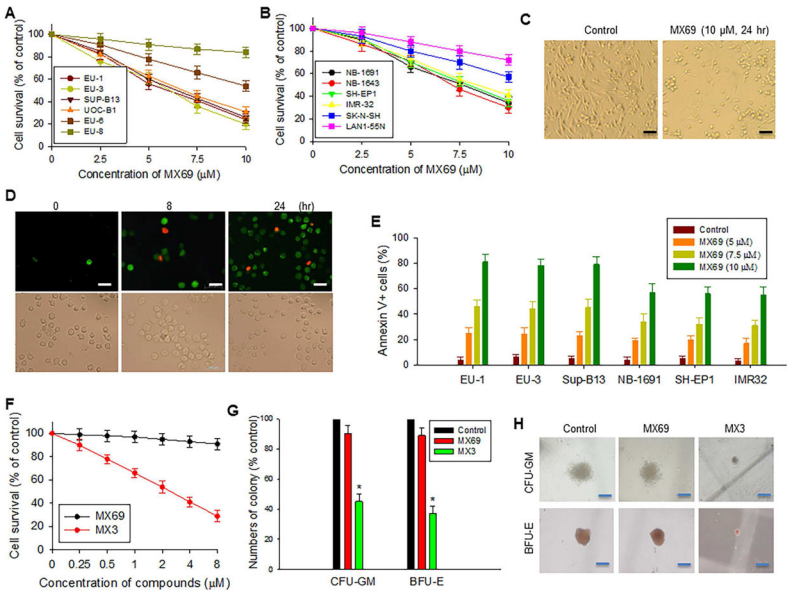

Figure 6.

Cytotoxic and apoptotic effects of leads on cancer and normal cells (A and B) WST assay for cytotoxic effect of MX69 on ALL (A) and NB (B) cells as indicated. Cells were treated for 24 hr. (C) Representative light microscopy photographs showing inhibition of NB-1691 cells treated by MX69 as compared to control. Scale bars, 10 μM. (D) Representative images showing induction of apoptosis (annexin V positive, green cells) and death (7-AAD positive, red cells) of EU-1 treated by 10 μM MX69. Scale bars, 10 μM. (E) ALL and NB cells were treated with MX69 doses indicated for 24 hr and apoptotic cells quantitatively detected by flow cytometry. (F) WST assay for cell survival of NBMM after 24-hr treatment with MX3 or MX69 at different concentrations. (G and H) comparison of inhibitory effects of MX3 and MX69 on CFU-GM and BFU-E in NBMM cells, using in vitro colony formation analysis. NBMM cells (1×10^5) were incubated with GM-CSF or Epo, with or without either 1 μM MX3 or 10 μM MX69. Colonies were counted after 14 days of culture. (G), comparison of colony numbers, *$p<0.01$. (H), comparison of representative colony sizes. Scale bars, 25 μM. Data in (A, B and F) represent mean ± SD of three independent experiments. Data in (E and G) represent mean of three independent experiments, bars ± SD. See also Figure S6 and Table S1.

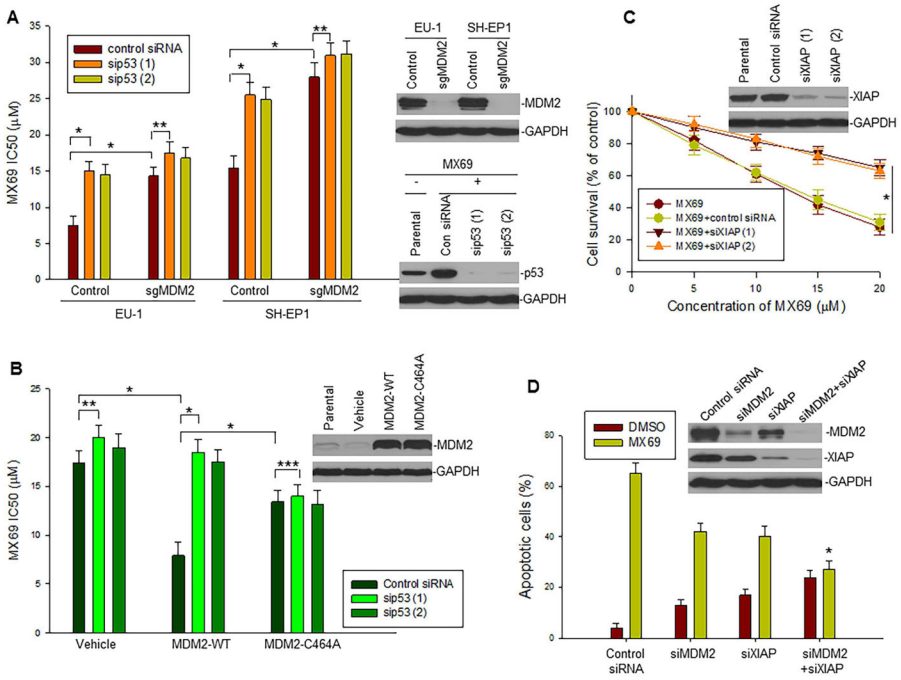

Figure 7.

Dependence of MX69-induced cell death on MDM2 and XIAP expression and p53 status

(A) Comparison of MX69 IC50 values in MDM2 KO (sgMDM2) EU-1 and SH-EP1 cells in presence or absence of sip53. IC50 values were measured by WST assay, *p<0.01, **p<0.05; Inserts, MDM2 and p53 expression in MDM2-silenced and MX69 and sip53-treated cells as detected by Western blot. (B) Comparison of MX69 IC50 values in SK-N-SH cells transfected with plasmids as indicated in presence or absence of sip53. IC50 values were measured by WST assay, *p<0.01, **p<0.05, ***p>0.5; Inserts, MDM2 expression in MDM2-transfected cells as detected by Western blot. (C) LA1-55N cells stably transfected with MDM2 in presence or absence of siXIAP were treated with MX69 (10 μM for 24 hr) and cell survival detected by WST assays; data represent mean ± SD of three independent experiments, *p<0.01; Insert, XIAP expression as detected by Western blot. (D) NB-1691 cells were treated with siMDM2, siXIAP (1), MX69 (10 μM for 24 hr) alone or their combinations as indicated and apoptotic cells quantitatively detected by flow cytometry, *p<0.05 (compared with siMDM2 or siXIAP alone); Insert, protein expression as detected by Western blot. Data in (A, B and D) represent mean ± SD of three independent experiments, bars ± SD. See also Figure S7.

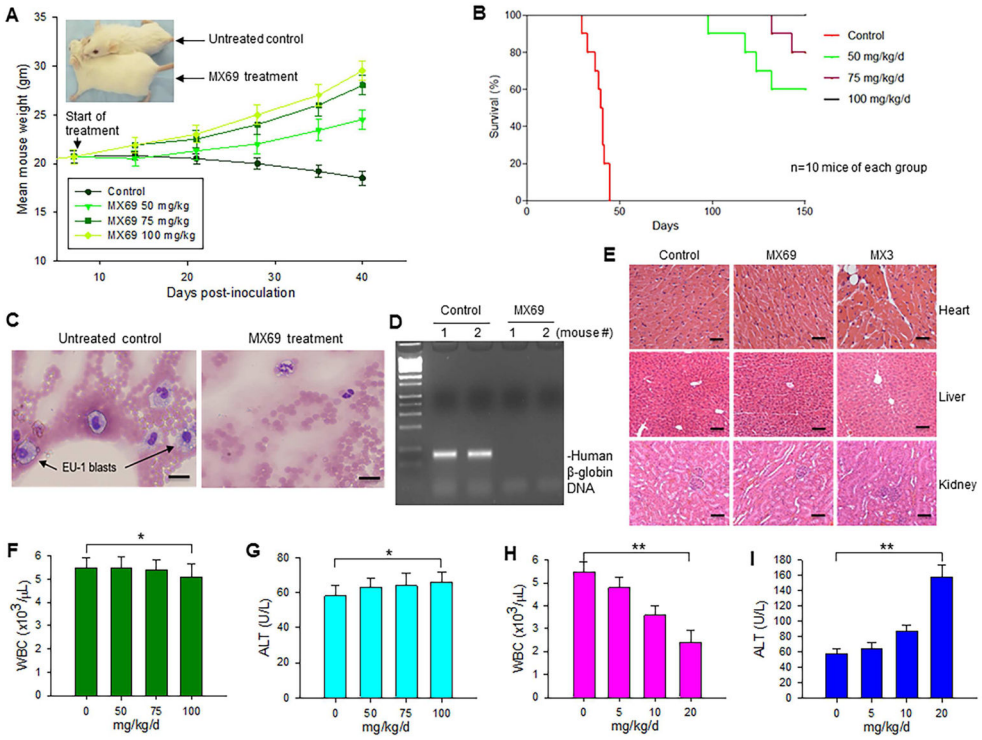

Figure 8.

The anti-cancer effect and toxicity of MX69 in vivo (A) Weight of SCID mice xenografted with EU-1 ALL cells and treated with MX69, as compared with the untreated control; data represent mean ± SD of 10 mice; Insert: size comparison of representative mouse from treatment and control groups, at 40-days post-treatment. (B) Comparison of EFS curves among each dose of MX69-treated groups and the control group of xenograft SCID mice. (C) Histological analysis of peripheral blood (Wright-Giemsa staining) of mice inoculated with EU-1 (left); and mice after treatment with MX69. Scale bars, 10 μM. (D) PCR for a 110-bp DNA fragment from the first exon of the human β-globin gene. (E) Representative histopathology of heart, liver and kidney of mice treated with 100 mg/kg/day of MX69 or 20 mg/kg/day of MX3. Scale bars, 25 μM. (F–I) Normal Hsd:ICR(CD-1) mice were treated with various doses of MX69 (F and G) or MX3 (H and I), as indicated in the schedule (3 days/week × 2), and then blood was collected and analyzed for the levels of WBC and ALT; data represent mean of three independent experiments, bars±SD, *p>0.5; ** p<0.01. See also Figure S8.